

SPATIAL-TEMPORAL DYNAMICS LAND USE/LAND COVER CHANGE AND FLOOD HAZARD MAPPING IN THE UPSTREAM CITARUM WATERSHED, WEST JAVA, INDONESIA

FAJAR YULIANTO ¹, SUWARSONO ¹, UDHI CATUR NUGROHO ¹,
NUNUNG PUJI NUGROHO ², WISMU SUNARMODO³, MUHAMMAD ROKHIS KHOMARUDIN ¹

¹Remote Sensing Application Center, Indonesian National Institute of Aeronautics and Space (LAPAN), Jakarta, Indonesia

²Research and Development Institute for Watershed Management Technology. Ministry of Environment and Forestry (KLHK), Jakarta, Indonesia

³Remote Sensing Technology and Data Center, Indonesian National Institute of Aeronautics and Space (LAPAN), Jakarta, Indonesia

Manuscript received: July 24, 2019

Revised version: February 20, 2020

YULIANTO F., SUWARSONO, NUGROHO U. C., NUGROHO N. P., SUNARMODO W., KHOMARUDIN M. R., 2020. Spatial-temporal dynamics land use/land cover change and flood hazard mapping in the Upstream Citarum watershed, West Java, Indonesia. *Quaestiones Geographicae* 39(1), Bogucki Wydawnictwo Naukowe, Poznań, pp. 125–146. 11 figs, 4 tables.

ABSTRACT: This study presents the information on the dynamics of changes in land use/land cover (LULC) spatially and temporally related to the causes of flooding in the study area. The dynamics of LULC changes have been derived based on the classification of Landsat imagery for the period between 1990 and 2016. Terrain surface classification (TSC) was proposed as a micro-landform classification approach in this study to create flood hazard assessment and mapping that was produced based on the integration of TSC with a probability map for flood inundation, and flood depth information derived from field observation. TSC as the micro-landform classification approach was derived from SRTM30 DEM data. Multi-temporal Sentinel-1 data were used to construct a pattern of historical inundation or past flooding in the study area and also to produce the flood probability map. The results of the study indicate that the proposed flood hazard mapping (FHM) from the TSC as a micro-landform classification approach has the same pattern with the results of the integration of historical inundation or previous floods, as well as field investigations in the study area. This research will remain an important benchmark for planners, policymakers and researchers regarding spatial planning in the study area. In addition, the results can provide important input for sustainable land use plans and strategies for mitigating flood hazards.

KEY WORDS: land-use/land-cover, flood hazard, remote sensing, Citarum watershed, West Java, Indonesia

Corresponding author: Fajar Yulianto, fajar.yulianto@lapan.go.id

Introduction

The hydrological cycle is also known as the water cycle, describing the phenomenon of the water recycling system on the earth, which is in the oceans, atmosphere, land surface, biosphere,

soil and groundwater systems. There are several stages of the hydrological cycle that occur on this earth, including evaporation and transpiration, precipitation, run-off and watershed processes (Narasimhan 2009, Marshall 2013, Inglezakis et al. 2016, Chakravarty and Kumar 2019). Water

contained in the sea and land surface can evaporate into the air and move up into the atmosphere directly and through vegetation as a process of evaporation and transpiration, that occurs condensation, clouds, and rain as a process of precipitation. Rainfall that falls to the ground surface becomes run-off, and also some water will be infiltrated into the ground and become ground water. The hydrological cycle process that occurs continuously on the surface of the earth is called 'watershed'. A watershed is an area that is bounded by surface topography and also drainage or river patterns. Rainfall that accumulates into the watershed will flow through drainage or river to an outlet on the surface of the earth (Marshall 2014, Muharomah 2014). Furthermore, the characteristics and conditions of a watershed in an area can be explained by a geomorphological approach. The geomorphological approach can describe and interpret the conditions of landforms on the surface of the earth that includes the nature of landforms, genesis, processes and material composition (Verstappen 1983, Panizza 1986, Huggett 2011).

Landuse/landcover (LULC) changes can impact the hydrological conditions such as land surface coefficient, discharge and hydrographic characteristics and also can affect the related run-off and infiltration characteristics and hydrological patterns in a watershed. An understanding of LULC changes is important in supporting decisions for global, regional and local land planning. LULC change analysis can reflect the dimensions, potential impacts and interactions of the relationship between human activity and the environment (Lambin 1997, Lopez et al. 2001, Dewan, Yamaguchi 2009, Armenteras et al. 2019). The rapid increase in the human population and the activities they undertake has consequences for LULC in terms of fulfilling their needs both socially and economically. Its development and the current and future conditions of water resources are very sensitive to LULC changes and the intensification of human activities (Alexakis et al. 2014, Yulianto et al. 2018). Various different human activities exert an influence on the hydrological cycle and water resources. These are directly related to land use for community and economic development, with LULC being an important indicator of these impacts. Indeed, LULC has a significant impact on the hydrological process and

the ecology of the watershed associated with run-off, in addition to evapotranspiration. Increased run-off as a result of LULC changes can affect the frequency of flooding, base flow and annual average flow in such a way as to alter the hydrological cycle (Birhanu et al. 2019, Fu et al. 2019, Yang et al. 2019). Flooding is the most frequent type of hydrometeorological disaster that occur in Indonesia. Flood events can cause problems such as the inundation of settlements, damage to infrastructure, disruption to community activities, health problems and loss of life and can create economic losses. Therefore, floods need to be anticipated in order to minimise the impact and risks that can result from such disasters (Yulianto et al. 2015).

Flood hazard assessment is one technique used in the creation of flood hazard mapping (FHM) or flood zoning areas aimed at reducing both flood risk and the impact of flooding. Flood hazard is influenced by various factors that can be grouped into hydrology and meteorology, geomorphology and LULC. Some of these factors are interrelated and provide a role in determining the FHM area (Bajabaa et al. 2013, Szwagrzyk et al. 2018). Hydrometeorology is an interdisciplinary field between meteorology and hydrology. Meteorological phenomenon, which is a weather event consisting of temperature, air pressure, water vapour and the gradient of the interaction of each variable in the atmosphere, can have influence on the hydrological cycle conditions. Weather forecasting can be used to predict the atmospheric conditions of a region in the future. This becomes an important part in hydrometeorological disaster mitigation efforts based on the scope of the watershed, such as floods, landslides, drought and others (Collier 2016, Botai et al. 2017). Watershed characteristics that exist on the surface of the earth as a process of the hydrological cycle can be identified and analysed through geomorphic processes related to landforms and also the surface material that is in the watershed. Study on environmental hazards is an applied geomorphology that examines hazards in the future or related to disasters in the past that have occurred. Identifying and analysing the process is an important aspect in the study of planning and management of a watershed area in an effort to reduce disaster risk (Panizza 1986, Goudie 2004, Gorum et al. 2008). Furthermore, changes in LULC can be

used as a benchmark in evaluating watershed responses related to flow hydrographs, which can be used to determine policy steps in handling hydrometeorological disasters in an area. Changes in hydrological properties depend on how large the level of LULC changes that occur in a watershed.

Several methods are used to create FHM, based on the hydrology, meteorology (e.g. Srivastava et al. 2013, Godfrey et al. 2015, Requena et al. 2015, Yucel et al. 2015, Dang, Kumar 2017, Afshari et al. 2018, Bass and Bedient 2018, Beretta et al. 2018) and geomorphology (e.g. Motevalli, Vafakhah

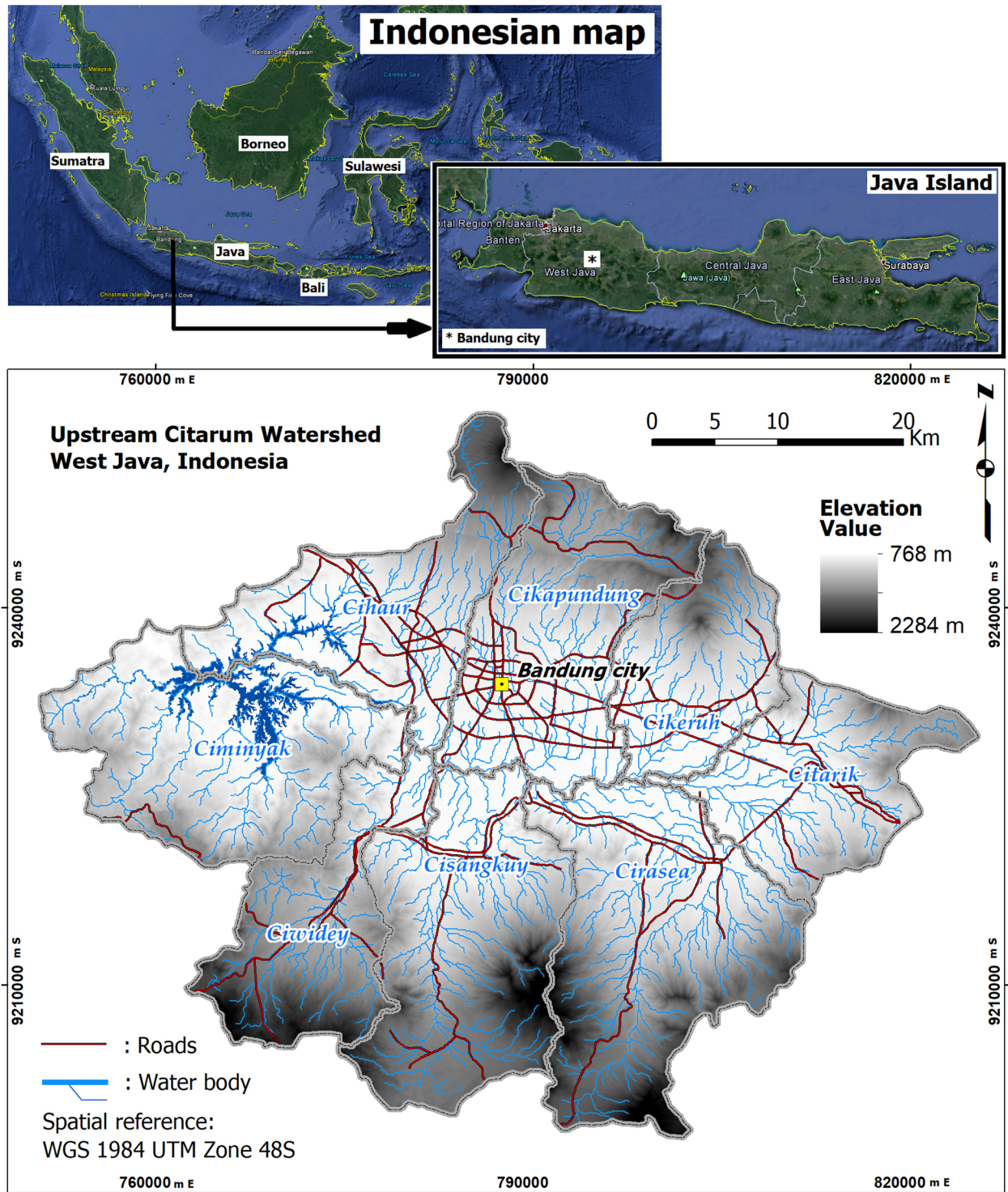


Fig. 1. Study area at the upstream Citarum Watershed, West Java, Indonesia. Elevation value from SRTM30 DEM provided by the U.S. Geological Survey (USGS).

2016, Righini et al. 2017, Samela et al. 2017, Langhammer, Vacková 2018, Mergili et al. 2018). Complex data are required for FHM based on a modelling with a hydrological and meteorological approach. These data include rainfall data, information on river flow, a cross section of the river and others. It can be difficult in developing countries and certain regional conditions to obtain the data needed for hydrological and meteorological modelling. The geomorphological approach may be used as an alternative to creating flood hazard assessments because of the inadequate, inaccurate and limited data for producing FHM using the hydrological and meteorological approach (Diakakis 2010, Ho et al. 2010, Ho, Umitsu 2011). The geomorphological approach can help in studying the extent of inundation, the direction of flood flows and changes in river channels through other evidence of flooding, the assistance of sedimentary features and deposits formed by repeated flooding, thus enabling an understanding of the nature/characteristics of former flood and the potential characteristics of floods that may occur in the future (Oya 2002, Lastra et al. 2008).

The study area (Fig. 1) is located in the upstream Citarum watershed, West Java, Indonesia, and consists of 8 (eight) sub-watersheds. These are Ciwidey, Cisangkuy, Cirasea, Citarik, Cikeruh, Cikapundung, Cihaur and Ciminyak. The area is also characterised by complex geomorphological variation, made up of plains, hills, mountains and valleys. The Bandung Basin area, or *Cekungan Bandung* (Fig. 2), is just one area of plains within the study area that is prone to flooding. There is a relationship between the Bandung Basin area and 8 sub-watersheds in the study area, which are based on river systems.

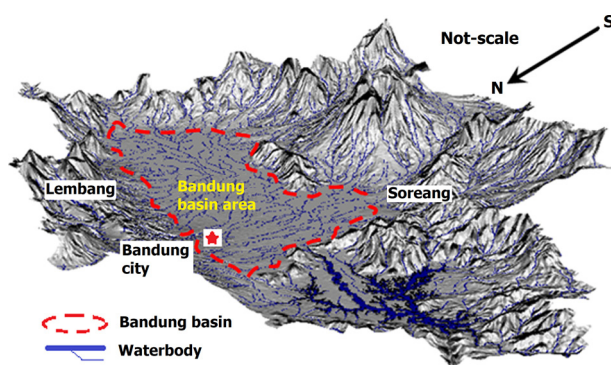


Fig. 2. 3D view of the SRTM30 DEM for the Bandung Basin area (Cekungan Bandung).

In the upstream Citarum, watershed starts from Situ Cisanti which is located in the southern part of Bandung Regency and Bandung City and flows northward into the Bandung Basin area. In this area, there are outlets of the 8 sub-watersheds in the upstream Citarum watershed, namely, Citarik from the East, Cikeruh from the North, Cikapundung from the North, Cihaur from the North, Cirasea from the South, Cisangkuy from the South, Ciwidey from the South and Ciminyak from the West. The flood frequency in the study area increased for the period 1931–2010 and at present, the condition is very critical. Such flood events have been greatly exacerbated in the recent years because of the massive increase in urban/built-up areas (Apip et al. 2010, Hudalah et al. 2010, Kartiwa et al. 2013, Dasanto 2014, Mulyo et al. 2018). Bandung city and its surrounding area have a higher economic growth rate than the national average. It has experienced many challenges because of the rapid pace of urbanisation, including slums; basic infrastructure; and flooding. There has been a gradual increase in urban development in the recent years.

Remote sensing and Geographic Information Systems (GIS) are powerful and cost-effective tools for analysing, monitoring and mapping the dynamics of LULC changes. In addition, the availability of multi-temporal data on processes and patterns is useful for analysis of FHM spatially and temporally (Zhang et al. 2002, Dewan, Yamaguchi 2009). For the reason, the study uses remote sensing and GIS techniques to observe the dynamics of LULC change, with the aim of identifying and mapping the flood hazard that underlies the development of Bandung city and its surrounding area. This research will become an important benchmark for planners, policy-makers and researchers regarding spatial planning in the study area. In addition, the results can provide important input for sustainable land use plans and strategies for mitigating flood hazards.

Materials and Methods

LULC Information

The input data for this study, comprising LULC maps information for 1990, 1996, 2000, 2003, 2009 and 2019, were collected from studies

conducted by Yulianto et al. (2018, 2019). The LULC information was obtained from 30-m multi-temporal Landsat imagery, which was classified using the maximum likelihood approach. There are 7 (seven) classes of LULC information, which are given as follows. Class 1, Urban/built-up area; Class 2, Primary forest; Class 3, Secondary forest and mixed garden; Class 4, Plantation; Class 5, Wet agricultural land; Class 6, Dry land farming; and Class 7, Water body. The maps and classes are presented in Fig. 3 and Table 1, respectively.

Interpretation related to forest classes, secondary forests and mixed gardens, plantations and several other classes on Landsat imagery can be performed based on the recognition of spatial character. The characteristics of these objects can be identified based on the interpretation elements such as colour, shape, size, pattern, texture, location and appearance associations of the object. The training area is needed in the classification process as a class identifier on the object. The training area can reflect the characteristics of each object to be classified. Furthermore, the maximum likelihood classification method has been used to classify LULC in the study area.

Specifically for urban/built-up area, primary forest, plantation, wet agriculture land, dry land farming and water body, classes can be distinguished based on the characteristics of colour, shape, size, pattern, texture, location and appearance of the object association. Meanwhile, the class of secondary forests and mixed gardens, based on their characteristics in Indonesia, tend to have similarities and mixed with other objects. Because of this mixing with several other objects, classification of the class becomes difficult. Thus,

in this study for the class, secondary forest and mixed garden are combined into one class.

Urban or Built-Up Area Expansion Rate

The urban area expansion rate (UAER) gives the average annual rate of growth of an urban or built-up area during a given period and can be formulated based on Equation (1) (Rimal et al. 2018, Rijal et al. 2018).

$$UAER = \frac{(UA_{t_2} - UA_{t_1})}{(T_{t_2} - T_{t_1})} \times 100 \quad (1)$$

where:

- UAER is the rate of urban area expansion (ha a^{-1}),
- UA_{t_1} and UA_{t_2} are the urban area sizes (ha) between times T_{t_1} and T_{t_2} in years, respectively.

Semi-automated Landform Classification

A landform, as a part of geomorphology, is the smallest unit of physical feature of the earth's surface that is produced by natural processes. Plains, hills, mountains and valleys are examples of features of the earth's surface that can be described as landforms. It is important to study and observe the characteristics of landforms and their relationship with human life in order to be aware of the potential hazards and disasters in a region. Landforms are characterised by differences in the structure and process of geomorphology, topography and constituent material (Strahler 1957, Verstappen 1983, Ruffell, McKinley 2014). In prior decades, the classification of landform properties has been carried out by calculating

Table 1. LULC descriptions used in this study (sourced and modified from Yulianto et al. (2018, 2019).

ID Class	LULC Type	Description
1	Urban/ built-up area	Consists of all built-up area, residential, industrial, commercial area, villages, settlements, transportation infrastructure and others.
2	Primary forest	Consists of natural forests that have not been disrupted by human exploitation.
3	Secondary forest and mixed garden	Consists of industrial plantation forests and some garden planting, coconuts, fruits and others.
4	Plantation	Consists of conservation land, tea plantation, palm oil and others.
5	Wet agricultural land	Consists of land that requires much water for its planting patterns: irrigated rice fields, rice terraces and others.
6	Dry land farming	Consists of land that requires little water for its cropping patterns: fields, moorland and others.
7	Water body	Consists of all water sources, rivers, reservoirs, ponds and others.

the geometry manually. Recently, however, an increase and expansion in computer technology has led to new spatial analysis methods, the development of algorithms and the ease of obtaining digital elevation data, all of which have

contributed to earth-oriented geomorphometrics (Tagil, Jenness 2008).

The development of computer technology has led to an acceleration in the processing of landform classification, which, in the past, was performed

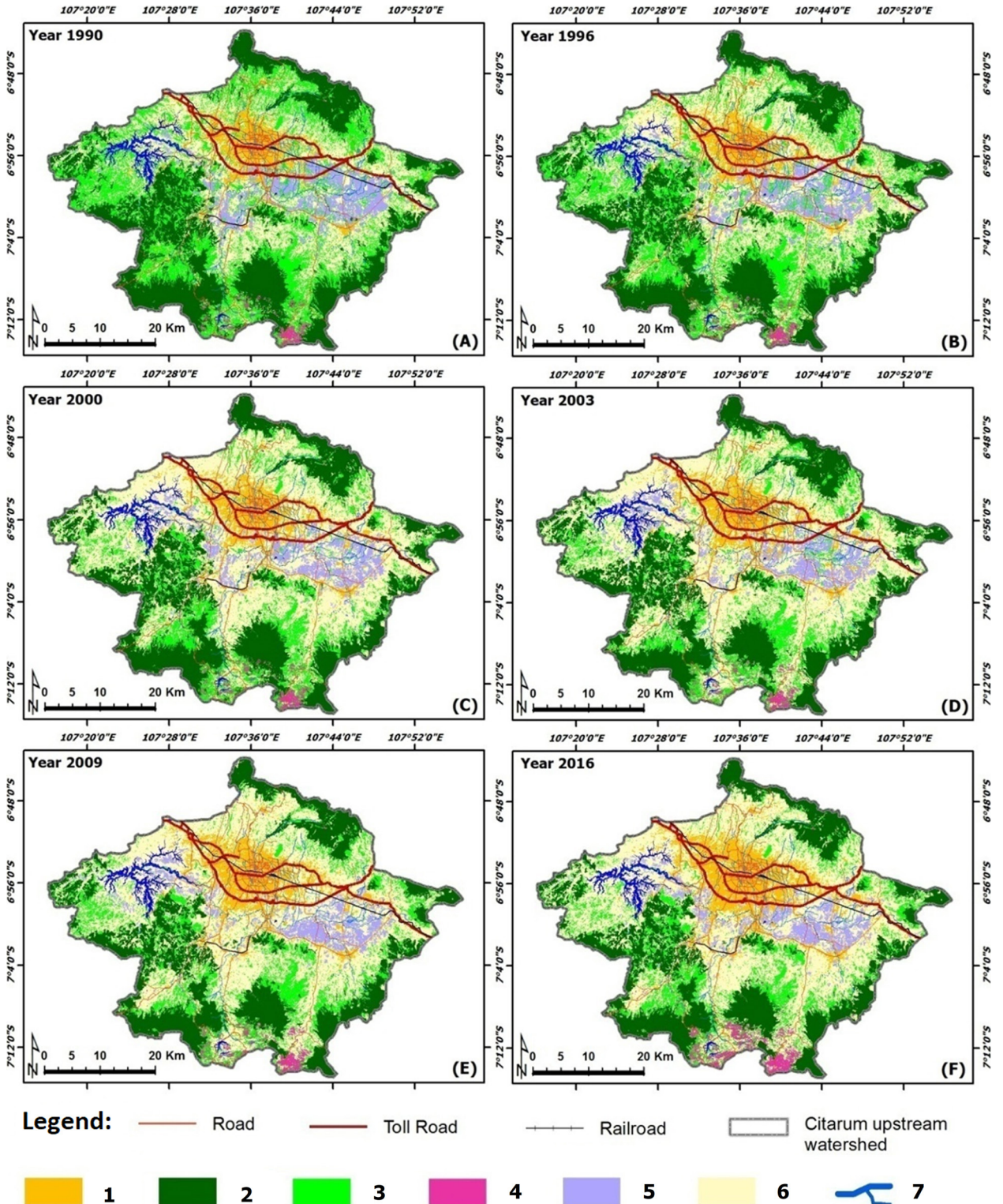


Fig. 3. LULC maps were used from various years during the period 1990–2016 (sourced and modified from Yulianto et al. (2018, 2019).

based on manual interpretation. Semi-automated landform-based classification is one such method that has both simplified and hastened the process of mapping and classification of landforms that was previously performed manually (e.g. Horton 1945, Coates 1958, Evans 1972). A GIS enables detailed analysis of land surfaces to be integrated by remotely sensed data, specifically digital elevation models (DEMs) (Schillaci et al. 2015). There are several methods of spatial analysis; the development of algorithms that contribute to earth-oriented geomorphometry include the curvature-based approach, fuzzy landform elements, pattern recognition, relief segmentation, object-based, morphometric feature and others. The development of these methods has thus helped to speed up the landform classification process (e.g. Irvin et al. 1997, Ehsani, Guisan et al. 1999, Burrough et al. 2000, Wilson, Gallant 2000, Weiss 2005, Ramalingan et al. 2006, Quiel 2008, Drăguț, Eisank 2012, Jasiewicz, Stepinski 2013).

Terrain surface classification (TSC) was used as the approach for the semi-automated landform classification in this study. TSC, as proposed by Iwahashi and Pike (2007), can be used to illustrate the geometric signature, comprising a set of measures that describe the shape of the topography by distinguishing geomorphologically different landscapes. Geometric signatures are designed to create an estimated terrain-unit map that includes slope gradient, surface texture and local convexity. In this study, the semi-automated extraction of landform elements that can be derived from SRTM30 DEM data was used to create a landform-based classification using the TSC approach. SRTM30 DEM was provided by the U.S. Geological Survey (USGS). System for Automated Geoscientific Analyses (SAGA) version 6.3 software was used to automatically identify the land elements from the TSC extraction (www.saga-gis.org). According to Olaya and Conrad (2009), SAGA is full-fledged GIS software whose features have some relation with geomorphometry. It also includes a large set of geoscientific algorithms that can serve as powerful tools in the analysis of DEMs.

Flood Hazards Assessment and Mapping

Ho and Umitsu (2011) conducted a research related to micro-landform classification and flood

hazard assessment and integrated the methods using remotely sensed data. The development of methods for the integration of the classification of micro-landforms and flood hazard zones was based on a geomorphological approach using SRTM30 DEM and Landsat data combined with field investigation. Flood hazard zonation was created based on categories from geomorphological features that grouped the average elevation of each landform into flood hazard classes. Furthermore, the results of their study to create flood hazard zonation were validated using field surveys, topographic characteristics and the history of flood inundation maps. This study has similarities in terms of the research topics that were examined by Ho and Umitsu (2011) related to flood hazard assessment and mapping. The difference with this study lies in the proposed use of the TSC approach to create micro-landforms as a basis for creating flood hazard assessment and mapping in the study area. The geomorphological characteristics in this case are represented by micro-landform units, whereas the flood characteristics and ground elevation level/value of each landform are used to analyse and classify the flood hazards in the study area. Other supporting data, such as flood height, were obtained from field surveys, whereas historical flood inundation data were procured from Sentinel-1 data in order to ascertain flood probability information.

Multi-temporal remotely sensed data for the period 2014–2018, Sentinel-1 C-band Synthetic Aperture Radar Ground Range Detected (SAR GRD), were used to create a flood probability map capable of describing the history of floods in the study area. According to Twele et al. (2016), Sentinel-1 data with Level-1 Ground Range Detected (GRD) products consist of focused SAR data that have been detected, multi-looked and projected to ground range using an earth ellipsoid model. Several data processing steps for Sentinel-1 SAR GRD products have been carried out in this study using SNAP version 6.0.0 developed by the European Space Agency (ESA), namely, (a) pre-processing, calibration; (b) pre-processing, speckle filtering; and (c) post-processing, geometric correction.

Flood inundations can be identified using the change detection approach based on before-flood and during-/after-flood information/

data available for the period 2014–2018. Implementation of the minimum error auto-thresholding algorithm was developed by Kittler and Illingworth (1986) and was used to classify flooding and non-flooding in the study areas. Field observations and interviews with residents of the surrounding area were conducted to gather information regarding the historical depth of the flood and the impact of the flood. Furthermore, flood probability can be calculated based on Equation (2).

$$Prob_total = \sum_{x=1}^y \frac{Prob_value_{x(i,j)}}{y} \quad (2)$$

where:

- *Prob_total* is the total flood probability value,
- *Prob_value_{x(i,j)}* is the probability value in various neighbourhood scenarios (*x*) (for *x* = 1, 2, 3, ..., *y*) in value for each pixel position (*i, j*).

Results

Change in LULC between 1990 and 2016

During the 26-year period of LULC observation from 1990 to 2016 (Fig. 4), LULC was dominated by dry land farming, primary forest, secondary forest and mixed garden, urban/built-up areas, wet agricultural land and plantation. Increases in LULC during this period occurred in urban/built-up areas, dry land farming and plantation. Meanwhile, decreases in LULC were recorded in respect of primary forest, secondary forest and mixed garden and wet agricultural land. For dry land farming during the period 1990–2016, the estimated change in area was an increase of 35,716 ha or 15.63%, whereas for urban/built-up areas and plantation, the increases were 11,374 ha (4.98%) and 3,097 ha (1.36%), respectively. Meanwhile, the estimated decreases

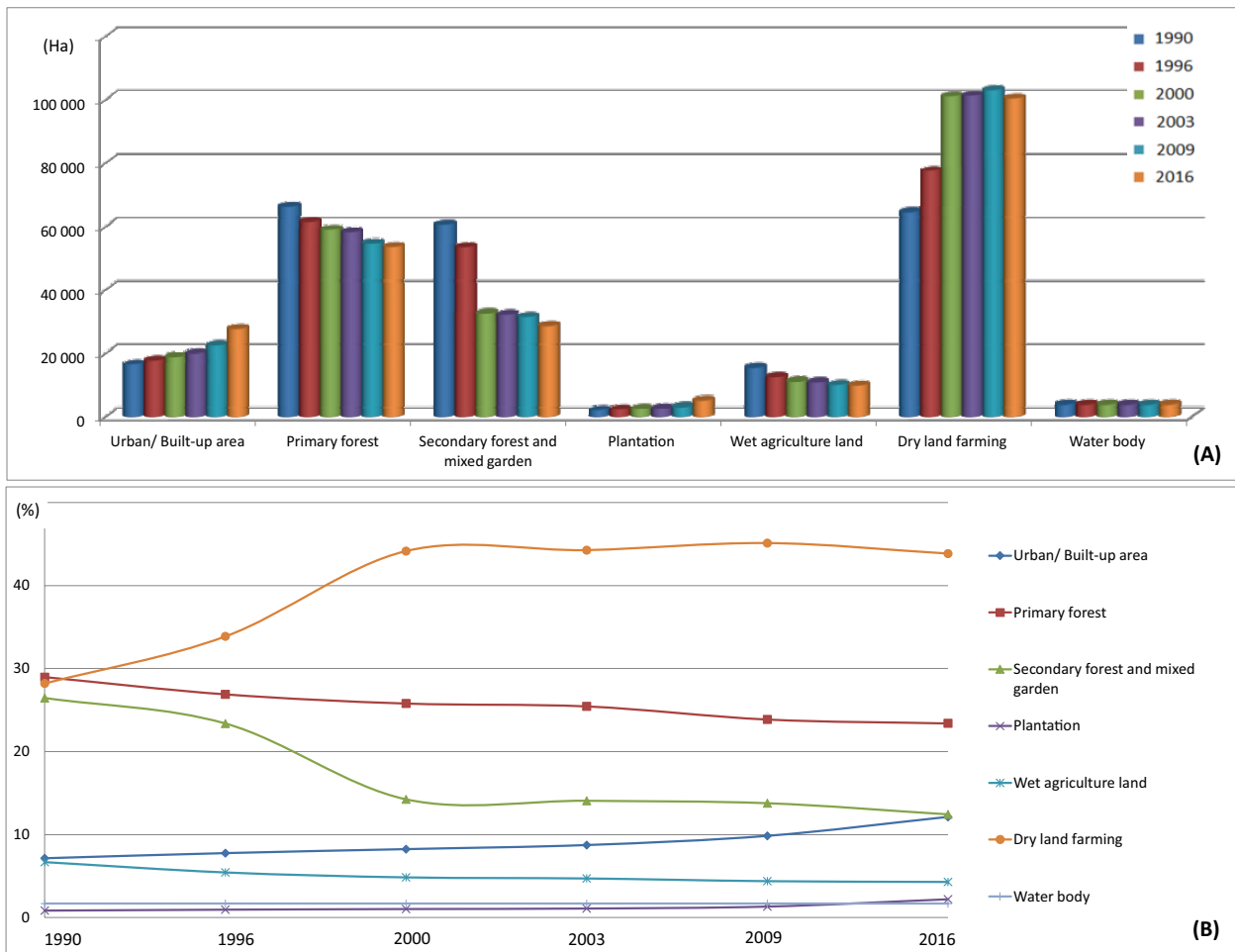


Fig. 4. The dynamics of LULC changes during the period 1990–2016 in the study area. A - estimated area in LULC changes (in hectares), B - Trends and percentages in LULC changes (in per cent).

in secondary forest and mixed garden, primary forest and wet agricultural farming were in the order of 32,018 ha (14.01%), 12,704 ha (5.56%) and 5,466 ha (2.39%), respectively.

Furthermore, the LULC distribution during the period 1990–2016 can be divided into eight sub-watersheds within the study area (Fig. 5), namely, Cihaur, Cikapundung, Cikeruh, Ciminyak, Cirasea, Cisangkuy, Citarik and Ciwidey. In order to analyse the role of LULC changes and their effects on flooding, the dynamics of changes in LULC calculations during 1990–2016 were detailed to the sub-watershed

level in the study area. Fig. 5 shows the distribution of the LULC classes within each sub-watershed. Cihaur, Cikapundung and Cikeruh are located in the northern part of Bandung, whereas Ciminyak, Cirasea, Cisangkuy, Citarik and Ciwidey are all located in the southern part of Bandung. In general, the primary forest class, as a rain catchment area, is better distributed in the southern part of Bandung than the northern part. Meanwhile, the distribution of areas in the urban/built-up area class, which have the potential to reduce the recharge area size, is concentrated in the northern part of Bandung

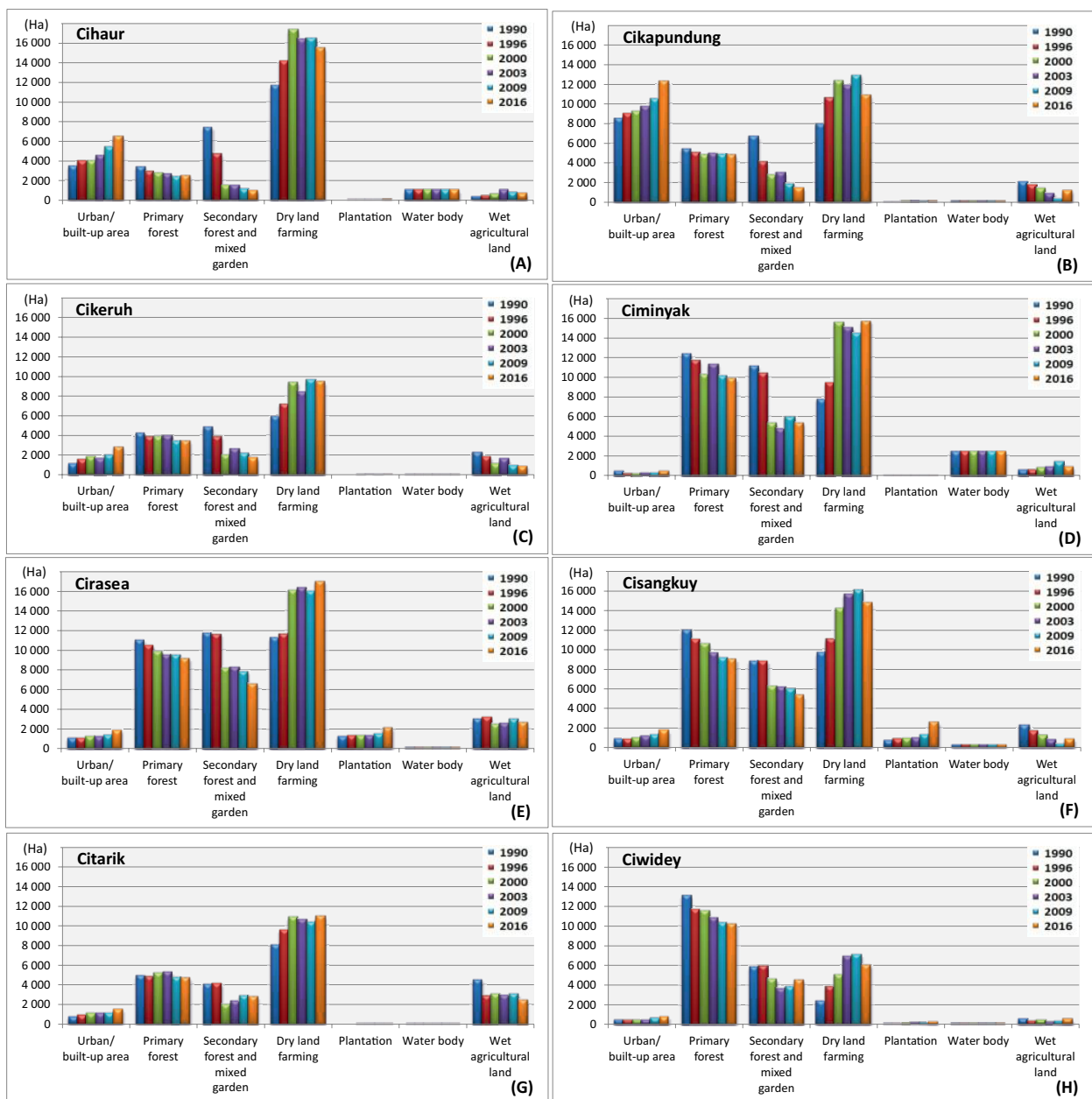


Fig. 5. The dynamics of LULC changes during 1990–2016 in the eight sub-watersheds in the study area.

in comparison to the southern part. During the period 1990–2016, there was an increase in the dry land farming class, which was distributed across all sub-watersheds and dominated the other classes.

Urban or Built-Up Area Expansion Rate

In addition to the primary forest that acts as a rain catchment area, the growth of urban/built-up areas can also lead to a reduction in the size of the catchment areas and thus contribute to flooding in the study area. The size of the urban/built-up areas and the rate of expansion of these areas across the eight sub-watersheds in the study area are presented in Tables 2 and 3. On the basis of Tables 2 and 3 and Fig. 6, it can be seen that of the eight sub-watersheds, three feature a high level and high rate of urban/built-up area expansion, namely, the Cikapundung, Cihaur and Cikeruh sub-watersheds located in the northern part of Bandung. The rates of urban/built-up area expansion for these 3 sub-watersheds during the period 1990–2016 were 149.9, 118.3 and 64.5 ha a⁻¹, respectively. Meanwhile, the sub-watersheds that had the rates of urban/built-up area expansion for 1990–2016 at or below 35.0 ha a⁻¹ are located in southern Bandung.

Semi-automated Landform Classification

The result of the semi-automated landform classification using the TSC approach in the study area is presented in Fig. 7. According to Iwahashi and Pike (2007), the parameters in TSC describe the geometric signatures used to create terrain-unit maps, which are related to slope gradient, surface texture and local convexity. In general, the micro-landform classification in the study area can be classified into 16 units. Furthermore, the Bandung Basin is used as a unit area boundary to enable a focus on the classification of potential flood areas. This is presented in Fig. 8 and combined with the information obtained using the Topographic Position Index (TPI) approach by Yulianto et al. (2019). Meanwhile, the use of TSC for micro-landform characteristics can be described in relation to flood conditions based on their characteristics, which is presented in Table 4.

Flood Hazard Assessment

On the basis of Table 4, TSC as a micro-landform classification approach displays characteristics in relation to flood conditions. There are 10 classes of TSC micro-landforms in the Bandung

Table 2. Urban/built-up area size in the eight sub-watersheds in the study area.

Sub-Watershed	Area (ha)					
	1990	1996	2000	2003	2009	2016
Cihaur	3,409.7	3,936.7	3,986.2	4,505.2	5,367.4	6,486.6
Cikapundung	8,414.6	8,965.7	9,222.3	9,702.7	10,451.0	12,311.6
Cikeruh	1,115.7	1,481.2	1,635.0	1,751.1	1,961.8	2,793.9
Ciminyak	207.1	210.3	218.8	292.9	422.2	435.3
Cirasea	1,019.8	1,022.3	1,194.9	1,257.6	1,373.7	1,788.1
Cisangkuy	808.3	858.7	944.5	1,111.6	1,318.9	1,692.9
Citarik	720.9	872.8	1,073.5	1,129.3	1,135.6	1,454.2
Ciwidey	391.9	392.8	405.1	459.9	586.6	753.9

Table 3. The rate of urban/built-up area expansion in the eight sub-watersheds in the study area.

Sub-Watershed	UAER (ha a ⁻¹)					
	1990–1996	1996–2000	2000–2003	2003–2009	2009–2016	1990–2016
Cihaur	87.8	12.4	173.0	143.7	159.9	118.3
Cikapundung	91.9	64.1	160.1	124.7	265.8	149.9
Cikeruh	60.9	38.4	38.7	35.1	118.9	64.5
Ciminyak	0.5	2.1	24.7	21.5	1.9	8.8
Cirasea	0.4	43.1	20.9	19.3	59.2	29.5
Cisangkuy	8.4	21.5	55.7	34.6	53.4	34.0
Citarik	25.3	50.2	18.6	1.1	45.5	28.2
Ciwidey	0.1	3.1	18.3	21.1	23.9	13.9

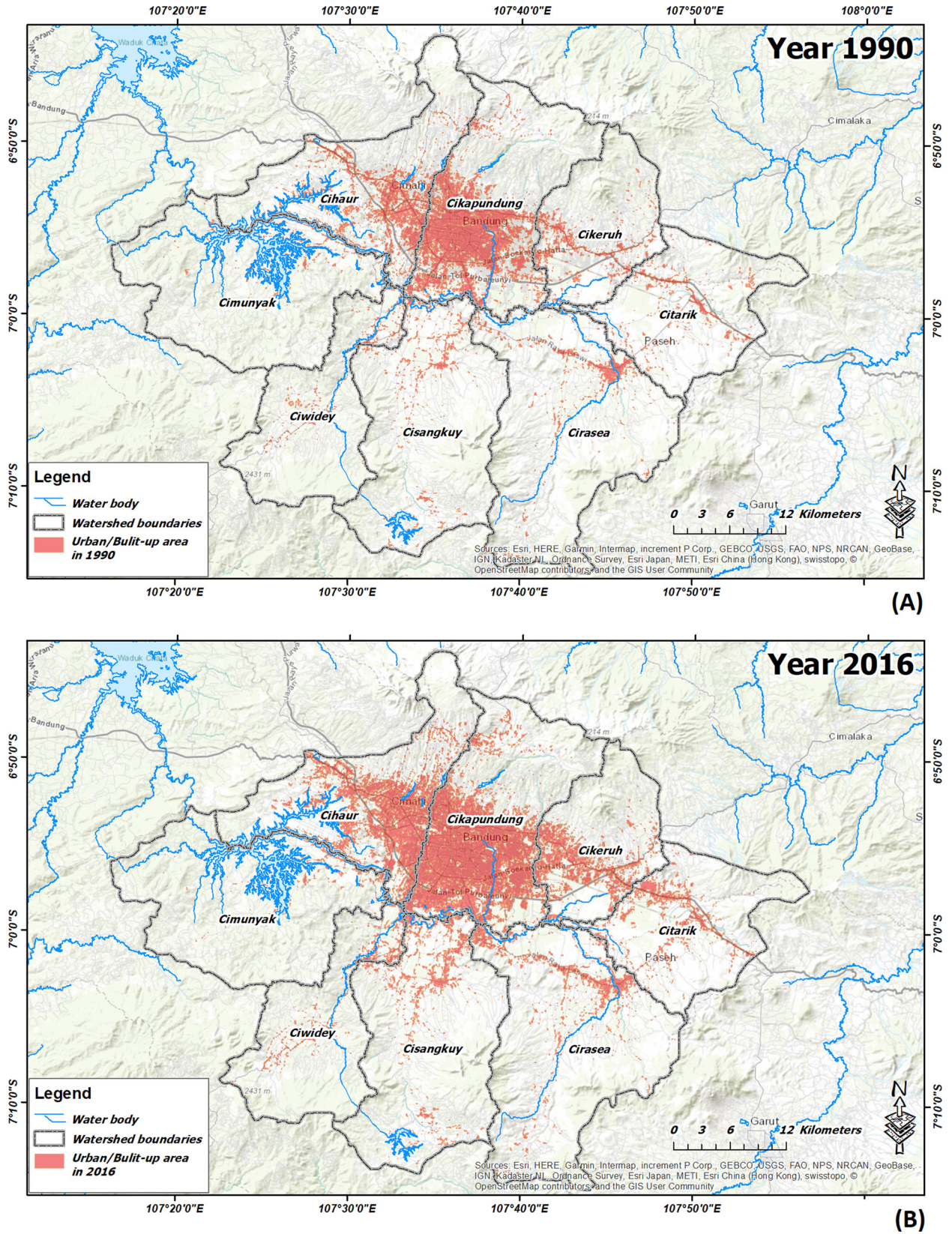
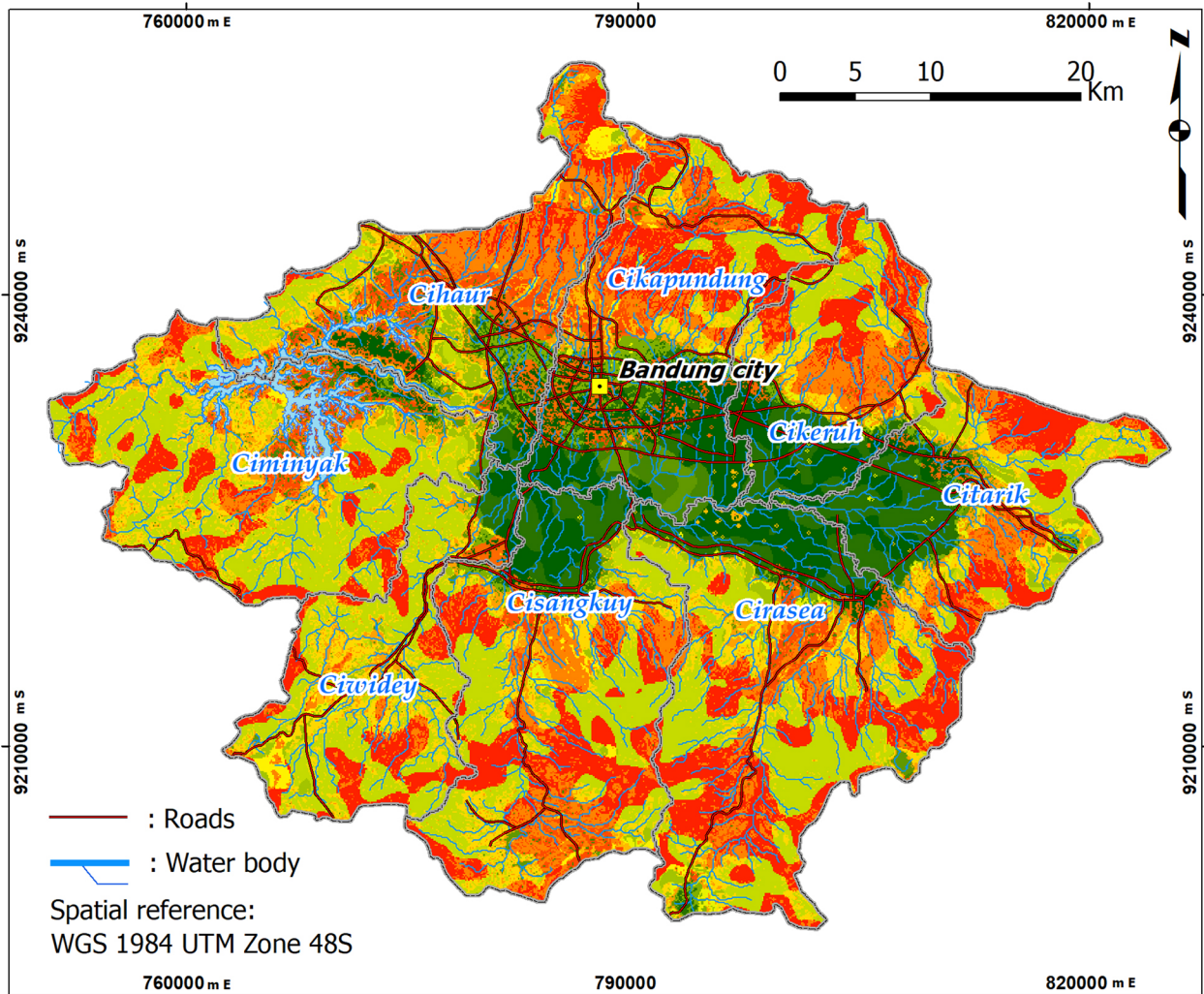


Fig. 6. Distribution of urban/built-up area expansion in the eight sub-watersheds in the study area in 1990 (A) and 2016 (B).



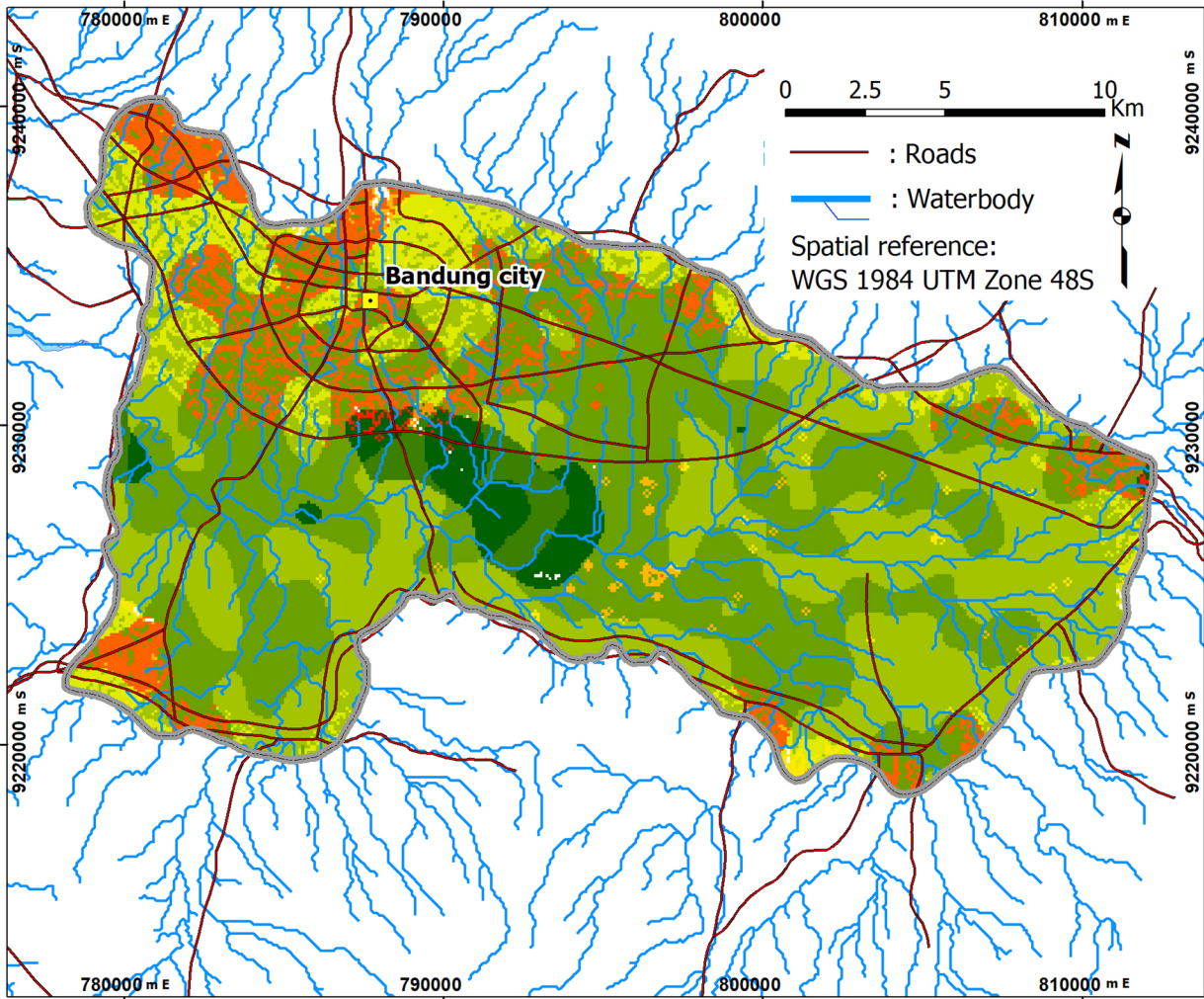
Legend

	Gentle slope, coarse texture, high convexity		Steep slope, coarse texture, high convexity
	Gentle slope, coarse texture, low convexity		Steep slope, coarse texture, low convexity
	Gentle slope, fine texture, high convexity		Steep slope, fine texture, high convexity
	Gentle slope, fine texture, low convexity		Steep slope, fine texture, low convexity
	Moderate slope, coarse texture, high convexity		Very steep slope, coarse texture, high convexity
	Moderate slope, coarse texture, low convexity		Very steep slope, coarse texture, low convexity
	Moderate slope, fine texture, high convexity		Very steep slope, fine texture, high convexity
	Moderate slope, fine texture, low convexity		Very steep slope, fine texture, low convexity

Fig. 7. Results of the terrain surface classification (TSC) as a micro-landform classification in the study area.

Basin, 8 of which are micro-landform classes that have the potential to be flooded based on their characteristics. Historical flood inundation data produced using multi-temporal Sentinel-1 data between 2014 and 2018 were used to analyse the probability of flood inundation in the study area, which is presented in Fig. 9. Field observations and interviews with residents of the surrounding area

were carried out to gather information regarding the historical depth of flooding and the impact of the floods. Furthermore, the results obtained from mapping the TSC as a micro-landform and the probability of inundation and flood depth taken from field observations have been integrated to produce maps and a flood hazard assessment of the study area, as presented in Fig. 10.



Legend

 Plains, Gentle slope, fine texture, high convexity	 Plains, Moderate slope, fine texture, low convexity
 Plains, Gentle slope, fine texture, low convexity	 Plains, Steep slope, fine texture, high convexity
 Plains, Gentle slope, coarse texture, high convexity	 Plains, Steep slope, fine texture, low convexity
 Plains, Gentle slope, coarse texture, low convexity	 Plains, Very steep slope, coarse texture, low convexity
 Plains, Moderate slope, coarse texture, high convexity	 Plains, Very steep slope, fine texture, high convexity

Fig. 8. Micro-landform classification uses the Bandung Basin as a unit area boundary to focus on classifying potential flood areas, which has been combined with information from the Topographic Position Index (TPI) approach by Yulianto et al. (2019).

Discussion

Effect of LULC changes related to flood contribution in the study area

The spatial distribution and analysis of LULC changes during the period 1990–2016 have shown an increase in some LULC classes that have the potential to reduce recharge areas and also contribute to flooding in the study area.

The expansion of the urban/built-up area class of 447.3 ha a⁻¹ during the period 1990–2016 has thus contributed to a reduction in recharge areas, especially in the northern part of Bandung (Fig. 6), where the greatest contributions came from the sub-watershed areas of Cikapundung, Cihaur and Cikeruh. This type of expansion also leads to an increase in run-off associated with the reduction of recharge areas in the study area. In addition, there has been a change in LULC class,

notably a shift towards dryland farming, which has come to dominate the other LULC classes and can also contribute to flooding in the study area. Some of the various types of plants used in dryland farming, such as potatoes, onions and others, tend to provide minimal vegetation cover and a high potential for erosion during rain that can affect the sedimentation and siltation of rivers in the study area. Reduced river capacity as a result of sedimentation tends to lead to the overflow of rivers and flooding. Meanwhile, the trend for year-on-year decreases in the coverage of both the primary forest and secondary forest and mixed garden class of LULC in the

area also impact on the reduction of infiltration zones, notably in the upstream areas of the study area. According to Rosyidie (2013), one cause of flooding in the study area was the change in LULC in those upstream areas that were previously forest and have since been converted into dry land farming, comprising horticultural farms with seasonal plants such as potatoes, carrots, mustard greens, cabbage and beans that tend to require a short time to harvest. High erosion rates occur because these seasonal plants do not protect the soil from erosion and contribute to sedimentation and flooding in the lower regions. Bosch and Hewlett (1982) described the strong

Table 4. Terrain surface classification (TSC) micro-landform characteristics related to flood conditions in the study area.

No	Micro-landform classification	Description	Flood hazard class
1	Plains, gentle slope, fine texture, high convexity	Plains area with the permissible range less than 9% gradient, dominant positive/concave convexity, fine texture indicates a high proportion of finer particles such as silt and clay. Depth of flooding in excess of 5 m	Very high flood hazard 1
2	Plains, gentle slope, fine texture, low convexity	Plains area with the permissible range less than 9% gradient, dominant negative/concave convexity, fine texture indicates a high proportion of finer particles such as silt and clay. Depth of flooding 4-5 m.	Very high flood hazard 2
3	Plains, gentle slope, coarse texture, high convexity	Plains area with the permissible range less than 9% gradient, dominant positive/concave convexity, coarse texture indicates a high proportion of sand. Depth of flooding 3-4 m.	High flood hazard 1
4	Plains, gentle slope, coarse texture, low convexity	Plains area with the permissible range less than 9% gradient, dominant negative/concave convexity, coarse texture indicates a high proportion of sand. Depth of flooding 2-3 m.	High flood hazard 2
5	Open slopes, moderate slope, coarse texture, high convexity	Open slope area with a gradient of slope between 10 and 15%, dominant positive/concave convexity, coarse texture indicates a high proportion of sand. Depth of flooding 1-2 m.	Moderate flood hazard 1
6	Open slopes, moderate slope, fine texture, low convexity	Open slope area with a gradient of slope between 10 and 15%, dominant negative/concave convexity, fine texture indicates a high proportion of finer particles such as silt and clay. Depth of flooding 1-2 m.	Moderate flood hazard 2
7	Upper slopes, steep slope, fine texture, high convexity	Upper slopes area with a gradient of slope between 16 and 30%, dominant positive/concave convexity, fine texture indicates a high proportion of finer particles such as silt and clay. Depth of flooding 0.5-1 m.	Low flood hazard 1
8	Upper slopes, steep slope, fine texture, low convexity	Upper slopes area with a gradient of slope between 16 and 30%, dominant negative/concave convexity, fine texture indicates a high proportion of finer particles such as silt and clay. Flood depth less than 0.5 m.	Low flood hazard 2
9	Upper slopes, very steep slope, fine texture, high convexity	Upper slopes area with a gradient of slope between 31 and 60%, and > 60%, dominant positive/concave convexity, fine texture indicates a high proportion of finer particles such as silt and clay.	No flood hazard 1
10	Upper slopes, very steep slope, coarse texture, low convexity	Upper slopes area with a gradient of slope between 31 and 60%, and > 60%, dominant negative/concave convexity, coarse texture indicates a high proportion of sand.	No flood hazard 2

correlation that exists between a reduction in forested areas, or deforestation, and an increase in flooding, whereas Wan and Yang (2007) explained how the expansion of urban/built-up areas is one of the major contributors to an increase

in flooding. Furthermore, Warburton et al. (2012) outlined how the contribution of LULC to flooding depends on the proportional and spatial distribution of various types of LULC within the watershed location. The results of this study (Fig.

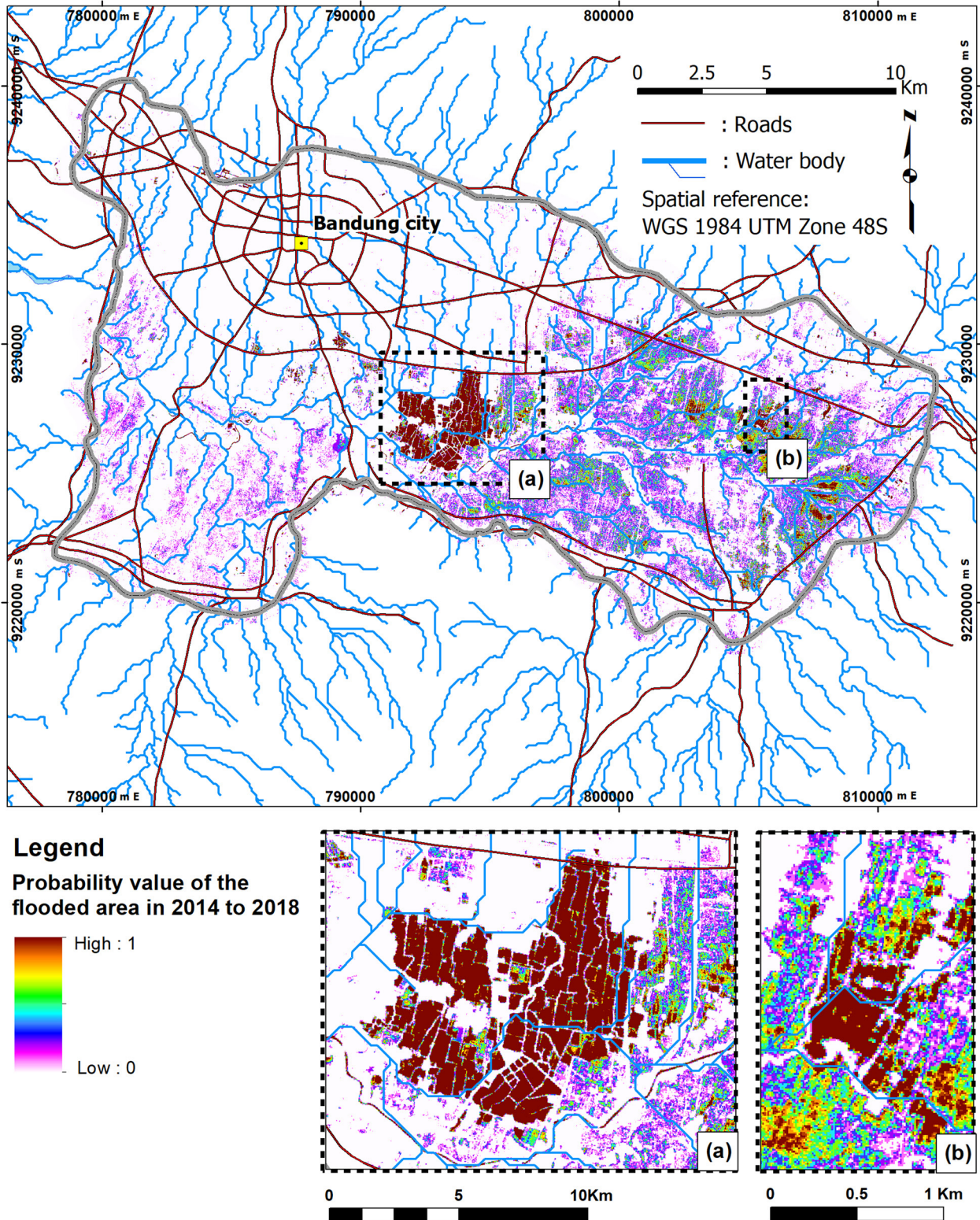


Fig. 9. Probability map for flood inundation from 2014 to 2018 in the study area.

5) show that the proportional distributions are different for each type of LULC in the sub-watersheds in the study area. The sub-watersheds of Ciwidey, Cisangkuy, Ciminyak and Cirasea are areas with the highest proportions of primary forest compared to the other sub-watersheds, which indicates that these areas remain relatively strong in terms of their catchment areas. Meanwhile, the sub-watersheds of Cikapundung, Cihaur, Cikeruh and Citarik contain more limited proportions of primary forest. This, coupled with relatively large proportions of urban/built-up areas and much in the way of dryland farming in these areas, tends to contribute significantly to flooding in the study area.

Flood hazard zone analyses and assessment

The result of the flood hazard assessment and mapping is based on the integration of TSC as a micro-landform classification approach with the flood inundation probability map and depth of flood data obtained from field observations (Fig. 10). In this study, the flood conditions and their interaction with micro-landform features are influenced by the topographic characteristics of the region in the form of the basin area, referred to collectively as the Bandung Basin or Cekungan Bandung. According to Narulita et al. (2008), the boundary of the Bandung Basin is an area based on the distribution of ancient Bandung lake sediments that morphologically formed a plain, with the surrounding area as the source of the lake sediment. This area is an ancient Bandung sedimentary plain that dried up thousands of years ago. The flooding mechanism in the study area is based on the topographic characteristics affected by the former lakes, alluvial fan plain and major river (i.e. the Citarum). The alluvial fan plain spreads to cover the northern part, and the river flows across the Bandung lake plain in meandering patterns, especially in the south of Bandung. The results of the flood hazard assessment map (Fig. 10) in the very high flood hazard class show the micro-landform of the study area in the form of a plain area with a slope of less than 9%, or gentle slope, which has high convexity (concave; for hazard 1) and low convexity (convex; for hazard 2) and is also characterised by the fine texture of sediment, the dominant proportion of which comprises finer particles such as silt and

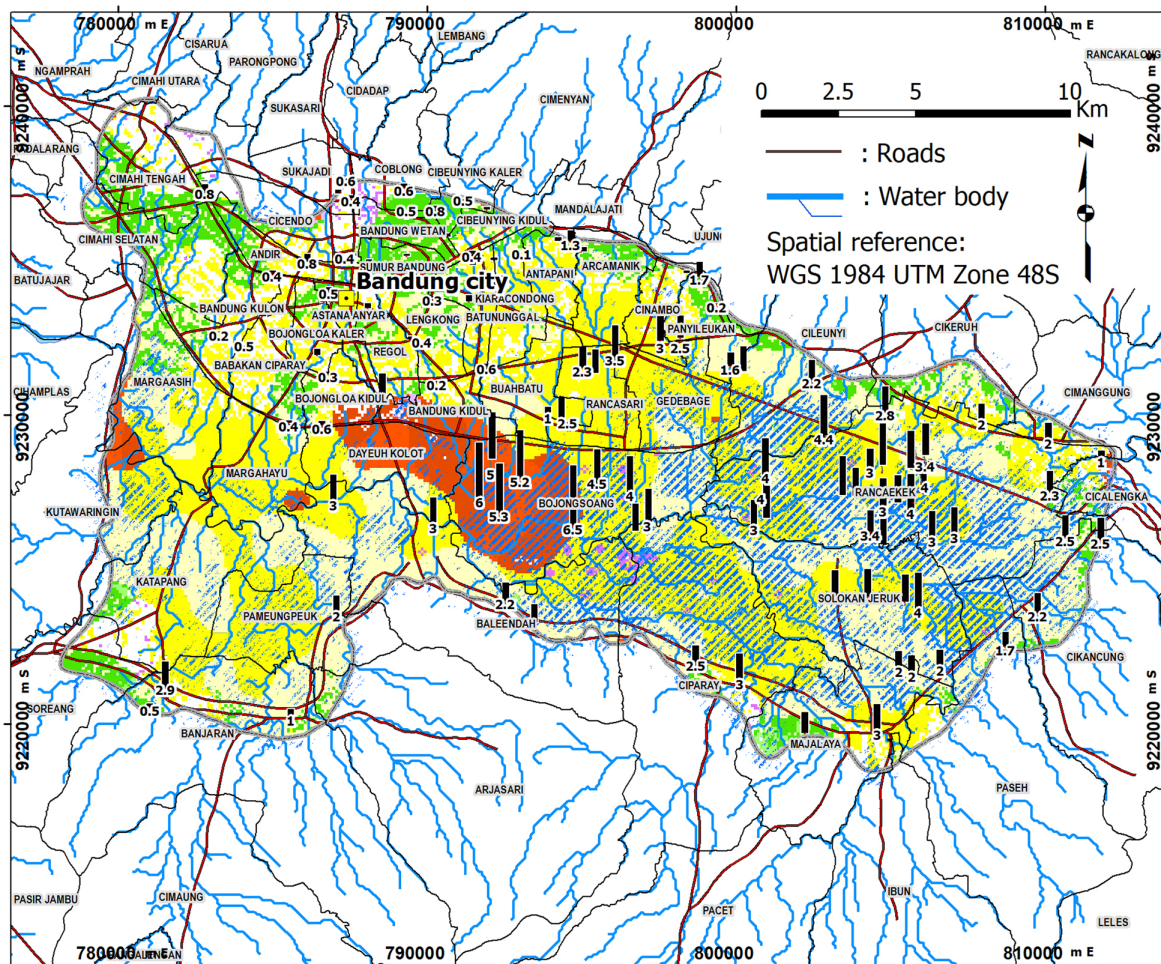
clay. The flood depth in the area is close to exceeding 5 m. Fig. 11a and 11b shows examples of locations in the very high flood hazard class located in the Baleendah district. Fig. 11c shows a location in the high flood hazard class and illustrates a micro-landform condition in the form of a plain featuring a gentle slope with coarse texture, thus indicating a greater composition of sand (compared to fine texture, dominantly clay) and which also has both high convexity (concave) and low convexity (convex). At this location in the Bojongsoang district, the depth of flood is between 2 and 4 m. Meanwhile, an example of a moderate hazard area location is given in Fig. 11d, which is located in Cibiroso, featuring a micro-landform class of open slopes, moderate slope, coarse texture, high convexity and a flood depth of 1–2 m. Hannan (2017) produced a map of potential flood hazards in the same location (in the study area) using the Topographic Wetness Index (TWI) approach. SRTM30 DEM data were also used as an input to calculate the flow accumulation and slope, which were then used to describe the wetness of the soil. According to Huang et al. (2008), Grabs et al. (2009) and Yang et al. (2015), TWI has a positive correlation with the characteristics of soil moisture, such as horizon depth, organic matter and clay content. Furthermore, TWI has been widely used to determine the wet conditions in a watershed and is able to identify areas that are saturated with water and thus have high flood potential. The results of the study by Hannan (2017) show that the TWI value in the study area ranged from -0.03 to 7.85 , which represents a large potential for flood disasters; this can then be classified as a map of potential flood hazards. This is in accordance with the results of this study, whereby the micro-landform areas with TSC classes of plain, gentle slope, fine texture and high convexity, and also those with low convexity, have very high flood hazard potential in accordance with the TWI value, which indicates a high wetness level. Meanwhile, regions that are characterised as being in the low flood hazard class have a TWI value indicating a low wetness level. Nurjaman (2018) used a GIS with the Complete Mapping Analysis (CMA) approach to identify the level of flood-prone parameters in the study area examined. The weighting method used to determine the score of each parameter was empirically based

on field observations and the number of flood events. The parameters used were slope, altitude, rainfall, soil texture, distance from the river, population density and land cover. The results of the study revealed that some of the sub-districts in the class that is very prone to flooding included Dayeuh Kolot, Rancaekek and Margahayu. Some of the locations included in flood-prone classes included Arjasari, Paseh and Baleendah, whereas locations that were not prone to flooding included Pengalengan, Pasir Jambu and Kertasari. The results show that the same thing related to

several locations with a flood-prone level, with the results of this study related to areas that range from the very high to low flood hazard classes in the study area.

Limitations and potential application

This study has analysed the description of LULC change information and its contribution to flooding in the study area. However, this study has not included a detailed quantitative analysis of the response of LULC changes to flooding. The



Legend

- Depth of flood (in meter)
- Field observations flood inundation point (historical)
- Past flood inundation in 2014 - 2018
- Very high flood hazard 1
- Very high flood hazard 2
- High flood hazard 1
- High flood hazard 2
- Moderate flood hazard 1
- Moderate flood hazard 2
- Low flood hazard 1
- Low flood hazard 2
- No flood hazard

Fig. 10. The result of flood hazard assessment and mapping based on the integration of TSC as a micro-landform classification approach, probability map for flood inundation and flood depths from field observation.

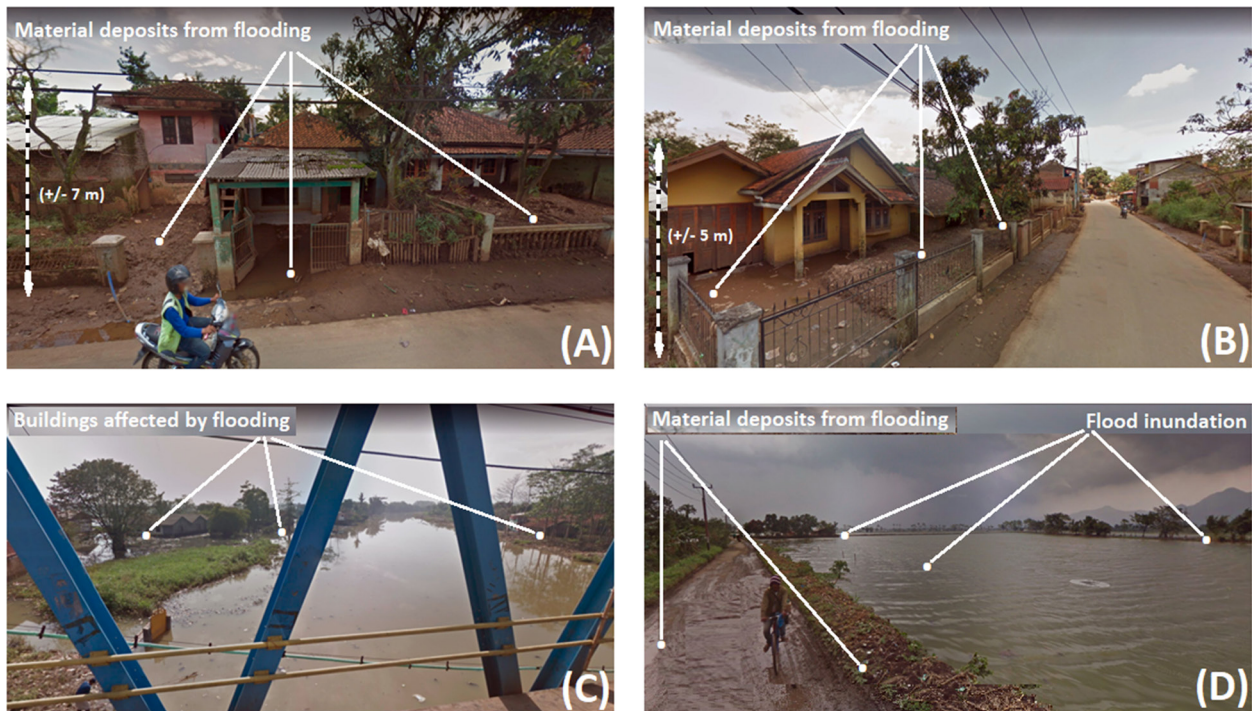


Fig. 11. Areas affected by flooding.

A, B - a very high flood hazard area in Baleendah, with TSC class of plains, gentle slope, fine texture, high convexity and a flood depth of more than 5 m. C - a high flood hazard area in Bojongsoang, with TSC class of plains, gentle slope, coarse texture, high convexity and a flood depth of 2-4 m. D - a moderate flood hazard area in Cibiroso, with TSC class of open slopes, moderate slope, coarse texture, high convexity and a flood depth of 1-2 m.

next study will conduct an analysis regarding this matter in order to determine the significant influence and contribution of LULC changes to flooding. The integration of TSC as a micro-landform classification approach, the probability map for flood inundation and the depth of flood data from field observation can be used as an alternative to developing flood mapping and hazard assessment. It would also be possible to apply these methods to other regions that have limited hydrological data and other parameters for the purpose of creating a flood hazard map as a basis for hydrological and meteorological modelling. This type of combined production related to flood hazards using various geomorphological, hydrological and meteorological approaches, in addition to several other approaches, is expected to yield more detailed and complete information. This study uses LULC information that was produced with Landsat multi-temporal data, along with SRTM30 DEM that can support scale mapping up to 1:50,000. The use of high-resolution satellite imagery and also high-resolution of digital elevation models (DEMs) will certainly produce more detailed information with respect

to producing LULC information and also for the use of TSC for a micro-landform area. In addition, this study has not included issues related to the environment, which also have an impact on the causes of floods in the study area. These issues include groundwater extraction and the phenomenon of land subsidence and deposition in the river sediment. As such, this constitutes an area for potential future research by adding parameters related to the issue in order to obtain more detailed and complete information.

Conclusion

This study used remote sensing and GIS techniques to understand the dynamics of LULC change and identify as well as undertake the FHM that underlies the development of Bandung city and its surrounding area. The decrease in the size of the areas of secondary forest and mixed garden, primary forest and wet agriculture is accompanied by, and closely related to, the expansion of urban/built-up areas and dry land farming, all of which were interpreted and classified

from multi-temporal Landsat imagery and purportedly result in reduced water infiltration into the soil, along with increased surface run-off as well as soil erosion. Therefore, they contribute to the occurrence of flooding in the Bandung Basin. Semi-automated landform classification using the TSC approach, based on 30-m SRTM DEM data, was successfully applied to the mapping of micro-landforms in a basin-shaped geomorphology. Likewise, Sentinel-1 data, a type of SAR with medium resolution, has the ability to map flood inundation in the geomorphological region. The integration of these two methods is very powerful for analysing flood hazard assessment. Integration of the LULC change analysis model with Landsat time series, medium-resolution optical data, semi-automated landform classification using the TSC approach based on SRTM30 DEM and analysis of historical flood inundation using multi-temporal Sentinel-1 SAR is a remote sensing and GIS approach that provides an effective and efficient means of understanding the dynamics of changes in LULC spatially and temporally and their relation to flood hazard in a basin area. This research will remain an important benchmark for planners, policymakers and researchers regarding spatial planning in the study area. In addition, the results can provide important input for sustainable land use plans and strategies for mitigating flood hazards. In future studies, the development of the results of this study can be used as an input for mapping and flood risk analysis, which will combine LULC, geomorphology and several other parameters.

Funding

This research was funded by the Program of National Innovation System Research Incentive (INSINAS) in 2019, Ministry of Research Technology and the Higher Education Republic of Indonesia. Contract No. 14/INS-1/PPK/E4/2019.

Acknowledgements

This article is a part of the research activities entitled 'The utilization of remote sensing data for disaster mitigation in Indonesia'. This research was funded by the Program of National Innovation System Research Incentive (INSINAS)

in 2019, Ministry of Research Technology and the Higher Education Republic of Indonesia. The authors thank Dr. Orbita Roswintarti as the Deputy Chairman for Remote Sensing Affairs of LAPAN, Dr. Dony Kushardono as the Group Leader in this activity, and the colleagues at the Remote Sensing Application Center of LAPAN for their discussions and suggestions. The authors thank the anonymous reviewers for their efforts and constructive comments that helped in improving the manuscript. SRTM30 DEM was provided by the U.S. Geological Survey (USGS). Sentinel-1 data were provided by Copernicus Open Access Hub, European Space Agency (ESA). The authors also extend their thanks to the Statistics Service Unit, Ministry of Communication and Information, West Java Province, Indonesia, for the discussion, collaboration, field surveys and sharing of spatial data to support this research.

Author Contributions

Conceptualization: FY, Methodology: FY, Data processing: FY, WS, Formal Analysis: FY, S, NPN, Validation: FY, S, UCN; Writing-Original Draft Preparation: FY, S, UCN, NPN, WS, MRK, Writing-Review & Editing: FY, S, UCN, NPN, WS, MRK.

References

- Afshari S., Tavakoly A.A., Rajib M.A., Zheng X., Follum M.L., Omranian E., Fekete B.M., 2018. Comparison of new generation low-complexity flood inundation mapping tools with a hydrodynamic model. *Journal of Hydrology* 556: 539–556. Doi: 10.1016/j.jhydrol.2017.11.036.
- Alexakis D.D., Grillakis M.G., Koutroulis A.G., Agapiou A., Themistocleous K., Tsanis I.K., Michaelides S., Pashiardis S., Demetriou C., Aristeidou K., Retalis A., Tymvios F., Hadjimitsis D.G., 2014. GIS and remote sensing techniques for assessment of land use change impact on hydrology: The case study of Yialis Basin in Cyprus. *Natural Hazards and Earth System Science* 14: 413–426.
- Apip, Takara K., Yamashiki Y., Ibrahim A.B., 2010. Assessment of spatially-distributed sediment budget and potential shallow landslide area for investment prioritization in sediment control of engaged catchment: A case study on the upper Citarum river, Indonesia. *Annals of Disaster Prevention Research Institute, Kyoto University* 53B: 45–59.
- Armenteras D., Murcia U., González T.M., Barón O.J., Arias J.E., 2019. Scenarios of land use and land cover change for NW Amazonia: Impact on forest intactness. *Global Ecology and Conservation* 17: e00567. Doi: 10.1016/j.gecco.2019.e00567.
- Bajabaa S., Masoud M., Al-Amri N., 2013. Flash Flood Hazard Mapping Based on Quantitative Hydrology, Geomorphology and GIS Techniques (Case Study of Wadi

- Al Lith, Saudi Arabia). *Arab Journal of Geosciences* 7: 2469–2481. Doi: 10.1007/s12517-013-0941-2.
- Bass B., Bedient P., 2018. Surrogate modeling of joint flood risk across coastal watersheds. *Journal of Hydrology* 558: 159–173. Doi: 10.1016/j.jhydrol.2018.01.014.
- Beretta R., Ravazzani G., Maiorano C., Mancini M., 2018. Simulating the influence of buildings on flood inundation in urban areas. *Geosciences* 8(2): 77. Doi: 10.3390/geosciences8020077.
- Birhanu A., Masih I., van der Zaag P., Nyssen J., Cai X., 2019. Impacts of land use and land cover changes on hydrology of the Gumara catchment, Ethiopia. *Physics and Chemistry of the Earth, Parts A/B/C*. Doi: 10.1016/j.pce.2019.01.006.
- Bosch J.M., Hewlett J.D., 1982. A review of catchment experiments to determine the effect of vegetation changes on water yield and evapotranspiration. *Journal of Hydrology* 55: 3–23.
- Botai C.M., Botai J.O., De Wit J.P., Ncongwan K.P., Adeola A.M., 2017. Drought Characteristics over the Western Cape Province, South Africa. *Water* 9: 876.
- Burrough P.A., van Gaans P.F.M., MacMillan R.A., 2000. High-resolution landform classification using fuzzy k-means. *Fuzzy Sets and Systems* 113: 37–52.
- Chakravarty P., Manoj Kumar M., 2019. Chapter 6 – Floral Species in Pollution Remediation and Augmentation of Micrometeorological Conditions and Microclimate: An Integrated Approach, *Phytomanagement of Polluted Sites*, Elsevier: 203–219. Doi: 10.1016/B978-0-12-813912-7.00006-5.
- Coates D.R. 1958. *Quantitative geomorphology of small drainage basins in Southern Indiana*. 1st Edn. New York: Columbia University
- Collier Ch.G., 2016. *Hydrometeorology*. Wiley Blackwell.
- Dang A.T.N., Kumar L., 2017. Application of remote sensing and GIS-based hydrological modelling for flood risk analysis: A case study of District 8, Ho Chi Minh city, Vietnam. *Geomatics, Natural Hazards and Risk* 8(2): 1792–1811. Doi: 10.1080/19475705.2017.1388853.
- Dasanto B.D., Boer R., Pramudya B., Suharnoto Y., 2014. Simple method for assessing spread of flood prone areas under historical and future rainfall in the upper Citarum watershed. *Environment Asia* 7(2): 79–86.
- Dewan A.M., Yamaguchi Y., 2009a. Land use and land cover change in Greater Dhaka, Bangladesh: Using remote sensing to promote sustainable urbanization. *Applied Geography* 29(3): 390–401. Doi: 10.1016/j.apgeog.2008.12.005.
- Dewan A.M., Yamaguchi Y., 2009b. Using remote sensing and GIS to detect and monitor land use and land cover change in Dhaka Metropolitan of Bangladesh during 1960–2005. *Environmental Monitoring and Assessment* 150(1–4): 237–249. Doi: 10.1007/s10661-008-0226-5.
- Diakakis M., 2010. A method for flood hazard mapping based on basin morphometry: Application in two catchments in Greece. *Natural Hazards* 56(3): 803–814. Doi: 10.1007/s11069-010-9592-8.
- Drăguț L., Eisank C., 2012. Automated object-based classification of topography from SRTM data. *Geomorphology* 141–142: 21–33.
- Ehsani A.H., Quiel F., 2008. Geomorphometric feature analysis using morphometric parameterization and artificial neural networks. *Geomorphology* 99: 1–12
- Evans I.S. 1972. General geomorphometry, derivatives of altitude and descriptive statistics. In: R.J.Chorley (ed.), *Spatial Analysis in Geomorphology*, New York: Harper and Row Publishers: 17–90.
- Fu Q., Shi R., Li T., Sun Y., Liu D., Cui S., Hou R., 2019. Effects of land-use change and climate variability on streamflow in the Woken River basin in Northeast China. *River Research and Applications* 35(2): 121–132. Doi: 10.1002/rra.3397.
- Godfrey A., Ciurean R.L., van Westen C.J., Kingma N.C., Glade T., 2015. Assessing vulnerability of buildings to hydro-meteorological hazards using an expert based approach – An application in Nehoiu Valley, Romania. *International Journal of Disaster Risk Reduction* 13: 229–241. Doi: 10.1016/j.ijdrr.2015.06.001.
- Gorum T., Gonencgil B., Gokceoglu C., Nefeslioglu H.A., 2008. Implementation of Reconstructed Geomorphologic Units in Landslide Mapping. *Natural Hazards* 46: 323–351.
- Goudie A.S. (ed.), 2004. *Encyclopedia of Geomorphology*. Routledge Taylor and Francis Group, New York.
- Grabs T., Seibert J., Bishop K., Laudon H., 2009. Modeling spatial patterns of saturated areas: A comparison of the topographic wetness index and a dynamic distributed model. *Journal of Hydrology* 373(1–2): 15–23. Doi: 10.1016/j.jhydrol.2009.03.031.
- Guisan A., Weiss S.B., Weiss A.D., 1999. GLM versus CCA spatial modeling of plant species distribution. *Plant Ecology* 143: 107–122.
- Hannan M.F.I., 2017. *Risk assessment and disaster mitigation directions flood in the Bandung basin area*. MS. Bogor Agriculture University (IPB), Indonesia
- Ho L.T.K., Umitsu M., 2011. Micro-landform classification and flood hazard assessment of the Thu Bon alluvial plain, central Vietnam via an integrated method utilizing remotely sensed data. *Applied Geography* 31(3): 1082–1093. Doi: 10.1016/j.apgeog.2011.01.005.
- Ho L.T.K., Umitsu M., Yamaguchi Y., 2010. Flood hazard mapping by satellite images and SRTM DEM in the Vugia – Thu Bon alluvial plain, central Vietnam. *International archive of the photogrammetry, remote sensing and spatial information sciences XXXVIII(8)*. Kyoto, Japan.
- Horton R.E., 1945. Erosional development of streams and their drainage basins: Hydrophysical approach to quantitative morphology. *Bulletin of the Geological Society of America* 56: 275–370.
- Huang X., Wang L., Yang L., Kravchenko A.N., 2008. Management effects on relationships of crop yields with topography represented by wetness index and precipitation. *Agronomy Journal* 100(5): 1463. Doi: 10.2134/ agronj2007.0325.
- Hudalah D., Winarso H., Woltjer J., 2010. Planning by opportunity: An analysis of periurban environmental conflicts in Indonesia. *Environment & Planning A* 42(9): 2254–2269.
- Huggett R.J., 2011. *Fundamentals of Geomorphology*. Routledge Taylor and Francis Group, New York.
- Inglezakis V.J., Pouloupoulos S.G., Arkhangelsky E., Zorpas A.A., Menegaki A.N., 2016. Chapter 3 – Aquatic Environment, *Environment and Development*, Elsevier: 137–212, Doi: 10.1016/B978-0-444-62733-9.00003-4.
- Irvin B.J., Ventura S.J., Slater B.K., 1997. Fuzzy and isodata classification of landform elements from digital terrain data in Pleasant Valley, Wisconsin. *Geoderma* 77: 137–154.
- Iwahashi J., Pike R.J., 2007. Automated classifications of topography from DEMs by an unsupervised nested-means algorithm and a three-part geometric signature. *Geomorphology* 86(3–4): 409–440. Doi: 10.1016/j.geomorph.2006.09.012.
- Jasiewicz J., Stepinski T.F., 2013. Geomorphons – a pattern recognition approach to classification and mapping of

- landforms. *Geomorphology* 182: 147–156. Doi: 10.1016/j.geomorph.2012.11.005.
- Kartiwa B., Murniati E., Bormudoi A., 2013. Application of hydrological model, RS and GIS for flood mapping of citarum watershed, West Java Province, Indonesia. *Journal of Remote Sensing Technology* 1(1): 1–8.
- Kittler J., Illingworth J., 1986. Minimum error thresholding. *Pattern Recognition* 19(1): 41–47. Doi: 10.1016/0031-3203(86)90030-0.
- Lambin E.F., 1997. Modeling and monitoring land-cover change processes in tropical regions. *Progress in Physical Geography* 21(3): 375–393.
- Langhammer J., Vacková T., 2018. Detection and mapping of the geomorphic effects of flooding using UAV photogrammetry. *Pure and Applied Geophysics* 175(9): 3223–3245. Doi: 10.1007/s00024-018-1874-1.
- Lastra J, Fernández E., Díez-Herrero A., Marquínez J., 2008. Flood hazard delineation combining geomorphological and hydrological methods: An example in the Northern Iberian Peninsula. *Natural Hazards* 45: 277–293.
- Lopez E., Bocco G., Mendoza M., Duhau E., 2001. Predicting land cover and land use change in the urban fringe a case in Morelia City, Mexico. *Landscape and Urban Planning* 55(4): 271–285.
- Marshall S.J., 2013. *Hydrology*. Reference Module in Earth Systems and Environmental Sciences. Doi: 10.1016/B978-0-12-409548-9.05356-2
- Marshall S.J., 2014. *The Water Cycle*. Reference Module in Earth Systems and Environmental Sciences. Doi: 10.1016/B978-0-12-409548-9.09091-6.
- Mergili M., Emmer A., Juřicová A., Cochachin A., Fischer J.T., Huggel C., Pudasaini S.P., 2018. How well can we simulate complex hydro-geomorphic process chains? The 2012 multi-lake outburst flood in the Santa Cruz Valley (Cordillera Blanca, Perú). *Earth Surface Processes and Landforms* 43(7): 1373–1389. Doi: 10.1002/esp.4318.
- Motevalli A., Vafakhah M., 2016. Flood hazard mapping using synthesis hydraulic and geomorphic properties at watershed scale. *Stochastic Environmental Research and Risk Assessment* 30(7): 1889–1900. Doi: 10.1007/s00477-016-1305-8.
- Muharomah R., 2014. Analisis run-off sebagai dampak perubahan lahan sekitar pembangunan underpass Simpang Patal Palembang dengan memanfaatkan teknik GIS. *Jurnal Teknik Sipil dan Lingkungan* 2(3): 424–433.
- Mulyo A., Haryanto A.D., Trirahardjo S., 2018. Korelasi hidrologi dan intensitas curah hujan daerah aliran sungai Cikampung: suatu pemahaman untuk mitigasi banjir di Kasawan Cekungan Bandung. Laporan Kemajuan Riset Kompetensi Dosen UNPAD.
- Narasimhan T.N., 2009. Hydrological Cycle and Water Budgets, *Encyclopedia of Inland Waters*, Academic Press: 714–720. Doi: 10.1016/B978-012370626-3.00010-7.
- Narulita I., Rahmat A., Maria R., 2008. Geographic information system application for determining regions rehabilitation priorities in the Bandung Basin. *Journal of Geology and Mining Research* 18(1): 23–35.
- Nurjaman A. (2018). Utilization of geographic information systems mapping of village areas in the area flow of Citarum river at Bandung district. MS. Bogor Agriculture University (IPB).
- Olaya V., Conrad O., 2009. Geomorphometry in SAGA. In: T.Hengl, H.I.Reuter (eds.), *Geomorphometry: Concepts, software, applications, Developments in Soil Science* 33: 293–308. Doi: 10.1016/s0166-2481(08)00012-3.
- Oya M., 2002. Applied geomorphology for mitigation of natural hazards. *Natural Hazards* 25(1): 17–25.
- Panizza M., 1986. *Environmental Geomorphology*. Amsterdam: Elsevier.
- Ramalingan S., Liu ZQ., Iourinski D., 2006. Curvature-based fuzzy surface classification. *IEEE Transactions on Fuzzy Systems* 14(4): 573–589.
- Requena A.L., Flores I., Mediero L., Garrote L. 2015. Extension of observed flood series by combining a distributed hydro-meteorological model and a copula-based model. *Stochastic Environmental Research and Risk Assessment* 30(5): 1363–1378. Doi: 10.1007/s00477-015-1138-x.
- Righini M., Surian N., Wohl E., Marchi L., Comiti F., Amponsah W., Borga M., 2017. Geomorphic response to an extreme flood in two Mediterranean rivers (north-eastern Sardinia, Italy): Analysis of controlling factors. *Geomorphology* 290: 184–199. Doi: 10.1016/j.geomorph.2017.04.014.
- Rimal B., Zhang L., Stork N., Sloan S., Rijal S., 2018. Urban expansion occurred at the expense of agricultural lands in the Tarai region of Nepal from 1989 to 2016. *Sustainability* 10: 1341.
- Rosydide A., 2013. Flood: Facts and effects, and the effects of land use change. *Journal of Urban and Regional Planning* 24(3): 241–249.
- Ruffell A., McKinley J., 2014. Forensic geomorphology. *Geomorphology* 206: 14–22. Doi: 10.1016/j.geomorph.2013.12.020.
- Samela C., Troy T.J., Manfreda S., 2017. Geomorphic classifiers for flood-prone areas delineation for data-scarce environments. *Advances in Water Resources* 102: 13–28. Doi: 10.1016/j.advwatres.2017.01.007.
- Schillaci C., Braun A., Kropáček J., 2015. Terrain analysis and landform recognition. In: L.Clarke, J.Nield, *Geomorphological techniques*, chap. 2, 4.2. Doi: 10.13140/RG.2.1.3895.2802.
- Srivastava P.K., Han D., Rico-Ramirez M.A., Islam T., 2013. Sensitivity and uncertainty analysis of mesoscale model downscaled hydro-meteorological variables for discharge prediction. *Hydrological Processes* 28(15): 4419–4432. Doi: 10.1002/hyp.9946.
- Strahler A.N., 1957. Quantitative analysis of watershed geomorphology. *Transactions, American Geophysical Union* 38(6): 913–920. Doi: 10.1029/tr038i006p00913.
- Szwagrzyk M., Kaim D., Price B., Wypych A., Grabska E., Kozak J., 2018. Impact of forecasted land use changes on flood risk in the Polish Carpathians. *Natural Hazards* 94: 227–240. Doi: 10.1007/s11069-018-3384-y.
- Tagil S., Jenness J., 2008. GIS-based automated landform classification and topographic, landcover and geologic attributes of landforms around the Yazoren Polje, Turkey. *Journal of Applied Sciences* 8: 910–921.
- Twele A., Cao W., Plank S., Martinis S., 2016. Sentinel-1-based flood mapping: A fully automated processing chain. *International Journal of Remote Sensing* 37(13): 2990–3004. Doi: 10.1080/01431161.2016.1192304
- Verstappen, H.Th., 1983. *Applied Geomorphology: Geomorphological Surveys for Environmental Development*. Amsterdam: Elsevier.
- Wan R., Yang G., 2007. Influence of land use/cover change on storm runoff—a case study of Xitiaoxi River Basin in upstream of Taihu Lake watershed. *Chinese Geographical Science* 17(4): 349–356.
- Warburton M.L., Schulze R.E., Jewitt G.P.W., 2012. Hydrological impacts of land use change in three diverse

- South African catchments. *Journal of Hydrology* 414–415: 118–135.
- Weiss A.D. 2001. Topographic position and landforms analysis. ESRI Users Conference, San Diego, CA, USA.
- Wilson J.P., Gallant J.C., 2000. Primary topographic attributes. In: J.P.Wilson, J.C.Gallant (eds.), *Terrain analysis: Principles and applications*, John Wiley & Sons, New York: 51–85.
- Yang L., Chen L., Wei W., 2015. Effects of vegetation restoration on the spatial distribution of soil moisture at the hill slope scale in semi-arid regions. *Catena* 124: 138–146. Doi: 10.1016/j.catena.2014.09.014.
- Yang W., Long D., Bai P., 2019. Impacts of future land cover and climate changes on runoff in the mostly afforested river basin in North China. *Journal of Hydrology* 570: 201–219. Doi: 10.1016/j.jhydrol.2018.12.055.
- Yucel I., Onen A., Yilmaz K.K., Gochis D.J., 2015. Calibration and evaluation of a flood forecasting system: Utility of numerical weather prediction model, data assimilation and satellite-based rainfall. *Journal of Hydrology* 523: 49–66. Doi: 10.1016/j.jhydrol.2015.01.042.
- Yulianto F., Maulana T., Khomarudin M.R., 2018. Analysis of the dynamics of land use change and its prediction based on the integration of remotely sensed data and CA-Markov model, in the upstream Citarum Watershed, West Java, Indonesia. *International Journal of Digital Earth* 12(10): 1151–1176. Doi: 10.1080/17538947.2018.1497098.
- Yulianto F., Sofan P., Zubaidah A., Sukowati K.A.D., Pasari-bu J.M., Khomarudin M.R., 2015. Detecting areas affected by flood using multi-temporal ALOS PALSAR remotely sensed data in Karawang, West Java, Indonesia. *Natural Hazards* 77(2): 959–985. Doi: 10.1007/s11069-015-1633-x.
- Yulianto F., Suwarsono S., Sulma S., 2019. Improving the accuracy and reliability of land use/land cover simulation by the integration of Markov cellular automata and landform-based models – a case study in the upstream Citarum watershed, West Java, Indonesia. *Journal of Degraded and Mining Lands Management* 6(2): 1675–1696. Doi: 10.15243/jdmlm.2019.062.1675.
- Zhang B.P., Yao Y.H., Cheng W.M., Zhou C.H., Lu Z., Chen X.D., 2002. Human-induced changes to biodiversity and alpine pastureland in the Bayanbulak Region of the East Tianshan Mountains. *Mountain Research and Development* 22: 1–7.